

Molecular Docking and QSAR Studies: Noncovalent Interaction between Acephate Analogous and the Receptor Site of Human Acetylcholinesterase

Khodayar Gholivand,^{*,†} Ali Asghar Ebrahimi Valmoozi,[†] Hamid R. Mahzouni,[†] Saied Ghadimi,[‡] and Rayhaneh Rahimi[†]

[†]Department of Chemistry, Tarbiat Modares University, P.O. Box 14115-175, Tehran, Iran

[‡]Department of Chemistry, Imam Hossein University, P.O. Box 16575-347, Tehran, Iran

S Supporting Information

ABSTRACT: Twelve new compounds of acephate (Ace) analogues were synthesized and characterized by ³¹P, ¹³C, and ¹H NMR and IR spectroscopy. The probable insecticide potential of these compounds as well as 23 previously prepared molecules with a general skeleton of RC(O)–NH–P(O)X₁X₂ was predicted by PASS software. Docking analysis showed that hydrophobic interaction and hydrogen bonding were created between the functional groups of Ace derivatives and the receptor sites of acetylcholinesterase. PCA–QSAR indicated that the electronic descriptors are dominated in comparison with the structural descriptors. The experimental–QSAR ($R^2 = 0.903$ and VIF < 2.997) and DFT–QSAR ($R^2 = 0.990$ and VIF ≤ 10) models clarified that the net charge of functional groups contributes an important function in an inhibition mechanism. Validity and integrity of this model were confirmed by the LOO cross-validation method with $q^2 = 0.940$ and low residuals between the training and testing sets. The correlation matrix of DFT–QSAR model confirmed the molecular docking results.

KEYWORDS: acetylcholinesterase inhibitors, docking, DFT calculation, QSAR

INTRODUCTION

Acephate (Ace) belongs to a class of insecticides known as phosphoramidothioates, which is widely used to eradicate agricultural pests.^{1–3} Its insecticidal potency and mammalian toxicity are attributed to the inhibition of the acetylcholinesterase (AChE) enzyme as a noncompetitive and reversible inhibitor.⁴ To clarify the inhibitory potency of Ace, the following investigations are present. Sokalski et al.,⁵ by using the ab initio analysis, suggested that the inhibition of AChE by Ace is a decomposition mechanism via the breakdown of a thiolester bond. Singh et al.^{6,7} illustrated that either phosphoryl or carbonyl interacts within the oxyanion–hole site. None of the two methods mentioned above are able to clarify this process at the molecular level. To extend and evaluate this issue, two new methods are introduced in order to overcome this problem. The quantitative structure–activity relationships (QSARs) approach has been used to investigate the possible interactions between Ace and AChE.^{8,9} Furthermore, integrated molecular docking has been performed to define a model for describing the interactions between them.¹⁰ The main steps for the development of a QSAR model could be summarized as: data preparation, data analysis, and model validation.¹¹ The appropriate molecular structural parameters computed by the density function theory (DFT) have been adopted to construct QSAR models.¹² The success of a QSAR model is highly dependent on the choice of effective descriptors.¹³ Principal component analysis (PCA) was used to detect the relationship between the dependent and independent variables and reducing the set of independent variables.^{12,14} Also, multiple linear Regression (MLR) and “leave-one-out” (LOO) cross-validation methods were used to find and validate the best

regression equation that is capable of correlating the changes in biological activities of the training and testing set compounds.¹⁵ In this study, we selected 35 insecticides (the probability of insecticide potential was predicted by PASS software) with the general skeleton of RC(O)–NH–P(O)X₁X₂. Compounds 24–35 as novel synthesized (Scheme 1) were synthesized and characterized by ³¹P, ¹³C, and ¹H NMR and IR spectroscopy, and the rest (1–23) (Table 1) had been previously prepared.^{16–19} Docking analysis and QSAR models (MLR, PCA data, and LOO cross-validation) were used to find the most efficient parameters, which can introduce a better mechanism of interaction between the selected molecules and the receptor site of human AChE.

MATERIALS AND METHODS

Calculations. The insecticide activity of these compounds was predicted by the prediction of activity spectrum for substances (PASS) software (version 1.193),²⁰ and molecular docking was used to obtain the ligand–protein interaction information. The calculations were carried out using the Protein Data Bank (PDB code: 1B41) file of huAChE enzyme and the AutoDock 4.2.3 package software.²¹ The stable geometry structures of compounds were further fully optimized using density functional theory (DFT) at the B3LYP/6-311+G** level of theory.²² Natural population analysis (NPA) was performed at the same level by using the Reed and Weinhold scheme.²³ All quantum chemical calculations were carried out by using the Gaussian 03 program package.²⁴ The correlation analysis was performed by the

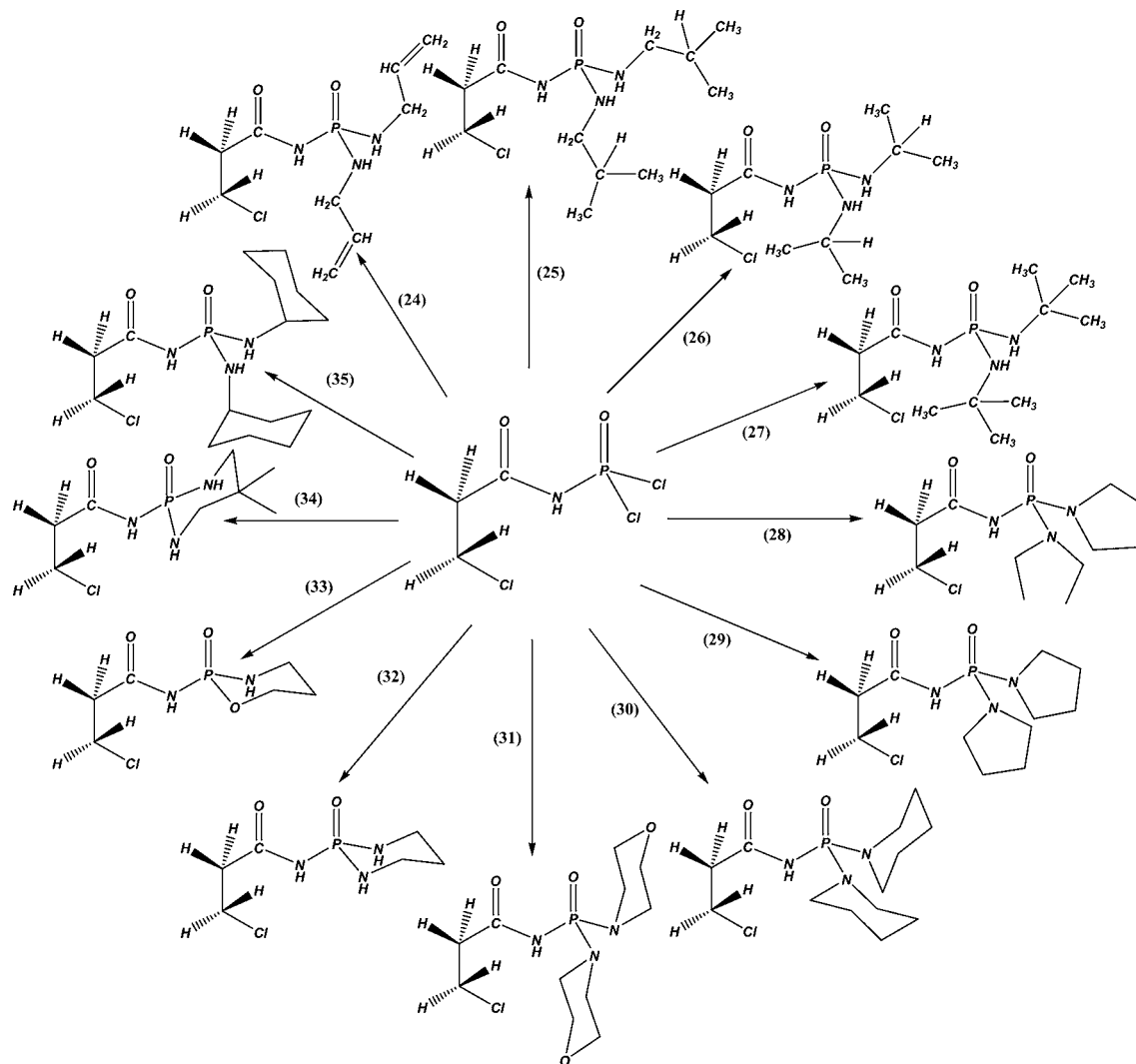
Received: March 14, 2013

Revised: June 20, 2013

Accepted: June 24, 2013

Published: June 24, 2013

Scheme 1. Preparation of Compounds 24–35



Statistical Package for Social Scientists (SPSS), version 16.0 for Windows.²⁵

Statistical Analysis. To identify the effect of physicochemical parameters on the AChE inhibition activity, QSAR studies were undertaken using the approach described by Hansch and Fujita.²⁶ The stepwise multiple linear regression procedure is a common method in QSAR studies for selection descriptors. MLR fits a linear model of the form (eq 1):

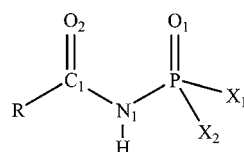
$$Y = b_0 + b_1X_1 + b_2X_2 + \dots + b_nX_k + e \quad (1)$$

where Y is dependent variable, X_1, X_2, \dots, X_k are independent variables (descriptors), e is a random error, and $b_0, b_1, b_2, \dots, b_k$ are known as the regression coefficients.²⁷

The electronic and structural descriptors (X) are obtained by either the quantum chemical calculations or experimental studies. The electronic descriptors include the energy of frontier orbitals (E_{HOMO} and E_{LUMO}), the energy difference between LUMO and HOMO ($\Delta E_{\text{L-H}}$), electrophilicity (ω),²⁸ polarizability (PL, the charge difference between the atoms in functional groups),²⁹ the net atomic charges (Q), and ^{31}P , ^{13}C , and ^1H NMR chemical shifts (δ).³⁰ Also, hydrophobic coefficient ($\log P$), dipole moment (μ), molecular volume (Mv), and molar refractivity (Mr) are the structural descriptors. E_{HOMO} , E_{LUMO} , ω , PL, Q , μ , and Mv values are obtained from the DFT results.³¹ The Mr is a constitutive-additive property that is calculated by the Lorenz–Lorentz formula.³² Also the logarithm of partition coefficient ($\log P$) is measured by the shake–flask method.³³ The calculated values of the descriptors are shown in Tables 1 and 2.

The toxicities (Y) of Ace analogues are expressed in terms of $\log(1/\text{IC}_{50})$ as an anti-AChE activity. The descriptor values were related with toxicity using MLR analysis. MLR of descriptors, selected for biological activity, give rise to the problem of multicollinearity. This problem can be solved by using the principal component analysis (PCA). These linear combinations form a new set of variables, namely principal components (PCs), which are mutually orthogonal. The first PC contains the largest variance and the second new variable contains the second largest variance, and so on.^{34,35} The variable selection in this PCA study was performed by using the Fisher's weights.²⁸ The descriptors with higher correlation coefficient and lower correlation ($|r| < 0.5$) to $\log(1/\text{IC}_{50})$ were selected to carry out stepwise MLR analysis and to optimize the QSAR equation.³⁶ The validity of the QSAR model was evaluated by LOO cross-validation method,³⁷ and an external data set was tested to evaluate the model. High square of the cross-validation coefficient (q^2) value in the training set shows only a good internal validation, but it does not automatically refer to its high validity for an external test set³⁸ because q^2 usually overestimates the validity of the model. Therefore, the QSAR model should be determined with a test set to confirm its validity. The performance of external validation was characterized by determination coefficient (R^2), standard error (S_{reg}), and q^2 , which are defined as follows, respectively (eqs 2–4):³⁹

$$R^2 = \frac{1 - \sum_{i=1}^n (y_i^{\text{fit}} - y_i)^2}{\sum_{i=1}^n (y_i - \bar{y})^2} \quad (2)$$

Table 1. Statistical Parameters of Physicochemical Properties and Experimental and Prediction of Anti-AChE Activity of the Ace Analogues for the Indicated Moiety

no.	Ace analogue		biological activity			physicochemical descriptors				
	R	X ₁ and X ₂	expt	PASS		electronic			hydrophobic	steric
			log(1/IC ₅₀)	anti-AChE	insecticide	δ ^{(31)P}	δ ^{(13)C₁}	δ ^{(1)H₁}	log P	Mr
1	CH ₂ Cl	Cl	0.201	0.180	0.298	6.62	167.12	9.16	-0.87	3.384
2	CHCl ₂	Cl	1.284	0.180	0.298	8.20	163.24	9.68	-0.48	3.186
3	CCl ₃	Cl	-0.580	0.399	0.559	8.08	160.30	9.94	-0.09	2.625
4	CF ₃	Cl	-0.380	0.397	0.388	7.42	157.50	10.24	-1.77	3.512
5	CH ₂ Cl	NC ₄ H ₈ O	-0.764	0.106		8.39	164.65	8.98	1.15	5.814
6	CHCl ₂	NC ₄ H ₈ O	-0.499	0.106		9.58	168.18	9.46	2.21	5.615
7	CCl ₃	NC ₄ H ₈ O	-0.764	0.228	0.364	9.51	168.61	8.59	2.91	5.060
8	CF ₃	NC ₄ H ₈ O	-1.187	0.227		8.44	162.65	9.20	1.59	5.941
9	H-C ₆ H ₄	Cl	-2.620	0.299	0.376	11.52	166.36	9.77	4.23	4.151
10	CH ₃ -C ₆ H ₄	Cl	-3.461	0.273	0.408	11.29	166.41	9.88	5.68	4.247
11	Cl-C ₆ H ₄	Cl	-2.768	0.245	0.405	11.41	165.42	9.91	5.21	4.240
12	Br-C ₆ H ₄	Cl	-2.792	0.168	0.313	11.48	165.81	9.89	6.55	4.225
13	H-C ₆ H ₄	NC ₄ H ₈ O	-2.585	0.179		10.83	165.51	8.41	1.32	4.151
14	CH ₃ -C ₆ H ₄	NC ₄ H ₈ O	-1.420	0.174	0.220	10.81	167.81	8.18	2.99	4.247
15	Cl-C ₆ H ₄	NC ₄ H ₈ O	-1.939	0.154	0.226	10.87	167.08	8.05	3.11	4.240
16	Br-C ₆ H ₄	NC ₄ H ₈ O	-1.757	0.091		10.81	166.08	8.82	3.54	4.225
17	CHCl ₂	NH-NC ₄ H ₈ O	-0.600	0.090		1.04	164.10	9.38	2.98	5.544
18	CF ₃	NH-NC ₄ H ₈ O	-0.931	0.223	0.245	0.32	157.50	10.11	2.96	5.633
19	CHCl ₂	NH-NC ₃ H ₁₀	-0.508	0.199		0.83	164.17	9.24	5.11	4.837
20	CCl ₃	NH-NC ₃ H ₁₀	-0.012	0.314	0.429	1.43	174.88	8.83	4.87	4.182
21	CF ₃	NH-NC ₃ H ₁₀	-0.448	0.313	0.286	2.52	157.27	9.83	5.09	4.926
22	C ₆ H ₅	NH-NC ₄ H ₈ O	-1.270	0.171	0.220	4.72	169.63	8.86	-0.78	5.513
23	C ₆ H ₅	NH-NC ₃ H ₁₀	-0.290	0.248	0.258	2.49	167.81	9.08	1.35	4.805

Table 2. Quantum-Chemical and Geometrical Descriptors for 19 Compounds Computed at 3LYP/6-311+G Level**

no.	electronic										hydrophobic	steric
	Q _F (au)	Q _{N(1)}	Q _{C(1)}	PL _{P=O}	PL _{C=O}	PL _{N-H}	E _{HOMO} (au)	E _{LUMO}	Δ _{L-H}	Ω	μ (Debye)	Mv (cm ³ /mol)
1	1.830	-0.995	0.674	-2.790	-1.204	-1.422	-0.313	-0.073	0.240	0.155	7.678	116.342
2	1.825	-0.984	0.657	-2.785	-1.187	-1.431	-0.310	-0.075	0.235	0.157	5.572	107.667
5	2.362	-0.984	0.670	-3.331	-1.254	-1.401	-0.254	-0.022	0.232	0.082	7.243	202.775
6	2.359	-0.966	0.651	-3.400	-1.207	-1.387	-0.251	-0.059	0.192	0.125	5.857	242.503
7	2.360	-0.962	0.651	-3.400	-1.187	-1.383	-0.252	-0.065	0.187	0.134	6.707	224.129
8	2.355	-0.948	0.600	-3.392	-1.143	-1.372	-0.252	-0.051	0.201	0.141	7.088	222.124
9	1.840	-0.996	0.682	-2.807	-1.242	-1.430	-0.273	-0.074	0.199	0.151	9.056	144.717
10	1.842	-0.997	0.682	-2.809	-1.245	-1.430	-0.265	-0.073	0.192	0.148	9.654	143.637
11	1.838	-0.995	0.682	-2.803	-1.240	-1.429	-0.270	-0.079	0.200	0.151	7.270	168.407
12	1.837	-0.994	0.681	-2.802	-1.240	-1.428	-0.266	-0.080	0.186	0.161	7.361	192.262
13	2.365	-0.969	0.676	-3.412	-1.260	-1.378	-0.247	-0.064	0.183	0.264	8.195	275.607
14	2.364	-0.972	0.680	-3.410	-1.271	-1.381	-0.247	-0.060	0.187	0.126	8.731	233.257
15	2.365	-0.968	0.675	-3.412	-1.258	-1.377	-0.248	-0.070	0.178	0.142	7.069	264.362
17	2.313	-0.951	0.649	-3.340	-1.212	-1.371	-0.255	0.060	0.195	0.127	5.027	279.269
18	2.305	-0.943	0.598	-3.326	-1.146	-1.369	-0.252	-0.058	0.194	0.124	5.819	260.377
19	2.315	-0.949	0.647	-3.342	-1.199	-1.373	-0.249	0.059	0.190	0.125	8.358	209.231
20	2.315	-0.949	0.647	-3.342	-1.199	-1.373	-0.249	-0.067	0.182	0.137	9.546	259.081
21	2.307	-0.940	0.597	-3.329	-1.148	-1.365	-0.250	-0.052	0.198	0.115	7.690	247.826
22	2.313	-0.958	0.676	-3.347	-1.282	-1.369	-0.253	-0.065	0.188	0.134	7.954	254.242

$$S_{\text{reg}} = \sqrt{\sum_{i=1}^n (y_i - \hat{y}_i)^2 / n - 1}$$

(3)

$$q^2 = 1 - \frac{\sum_{i=1}^{n_{\text{EXT}}} (y_i - \hat{y}_i)^2}{\sum_{i=1}^{n_{\text{EXT}}} (y_i - \bar{y}_{\text{EXT}})^2}$$

(4)

where y_i^{fit} is the fitted log ($1/IC_{50}$) value of the i th compound, \bar{y} is the average response value in the training set, y_i and \hat{y}_i are the observed and predicted values for the i th compound, respectively. \bar{y}_{EXT} is the average response value of the validation set, n stands for the number of compounds in the training set, and n_{EXT} is the number of compounds in the validation set.

Synthesis. ^1H , ^{13}C and ^{31}P NMR spectra were recorded on a Bruker Avance DRX 500 spectrometer. ^1H and ^{13}C chemical shifts were determined relative to internal TMS, and ^{31}P chemical shifts relative to 85% H_3PO_4 as the external standard. Infrared spectra were recorded on a Shimadzu model IR-60 spectrometer using KBr pellets. Melting points of compounds were obtained with an electrothermal instrument. UV spectrophotometer was performed using a PERKIN-ELMER Lambda 25. *N*-3-Chloropropylphosphoramidic dichloride as starting material was prepared according to the literature methods,^{16–19} and other phosphoramidic derivatives were synthesized as follows (Scheme 1):

Compounds 1–23 as previously synthesized (PS) and compounds 24–35 as novel synthesized (NS) were prepared by the reaction of 1 mmol (0.193 g) of the phosphoric dichloride derivatives with 4 mmol (0.228 g) of the corresponding amines in dry acetonitrile (40 mL). The phosphoric dichloride derivatives were added dropwise to a mixture while stirring. The temperature was controlled in the range -5 to -8 °C. After stirring for 6 h, the precipitate was filtered and the product was washed using distilled water.

Enzymatic Experiments. Human AChE activity measurements were performed essentially according to the method of Ellman.⁴⁰ The reaction was carried out at 37 °C in 70 mM phosphate buffer ($\text{Na}_2\text{HPO}_4/\text{NaH}_2\text{PO}_4$, pH = 7.4) containing the AChE enzyme (10 μL volume, diluted 100 times in phosphate buffer, pH = 7.4), DTNB (5,5'-dithiobis(2-nitrobenzoic acid)) (10^{-4} M concentration), and ATCh (1.35×10^{-4} M concentration). Each compound was dissolved in dimethyl sulfoxide (DMSO) and then added to buffer for in vitro cholinesterase assays. The highest concentration of DMSO used in the assays was 5%. In independent experiments without the inhibitor, 5% DMSO had no effect on the inducing activity of enzyme. The absorbance change at 37 °C was monitored with the spectrophotometer at 412 nm for 3 min, and three replicates were run in each experiment. In the absence of inhibitor, the absorbance change was directly proportional to the enzyme level. The reaction mixtures for determination of IC_{50} values, the median inhibitory concentration, consisted of DTNB solution, 100 μL , inhibitor, x μL , acetylthiocholinidide (ATCh) solution, 40 μL , phosphate buffer (850- x) μL , and hAChE solution, 10 μL . The plot of V_i/V_0 (V_i and V_0 are the activity of the enzyme in the presence and absence of inhibitors, respectively) against $\log[I]$ (where, $[I]$ is the inhibitor's concentration) gave the IC_{50} values of five compounds 27–31 (Figure 1).

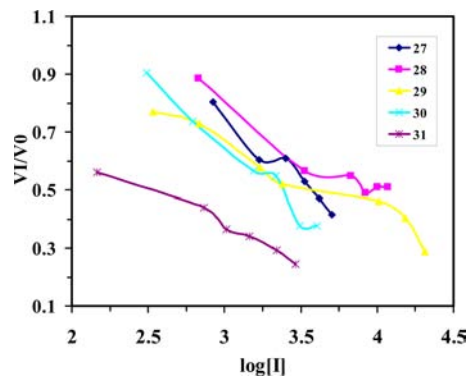


Figure 1. The plot of V_i/V_0 against $\log[I]$ for inhibitors 27 (black line with \blacklozenge), 28 (magenta line with \blacksquare), 29 (yellow line with \blacktriangle), 30 (cyan line with \times), and 31 (violet with $*$); V_i and V_0 are the AChE enzyme's activity in the presence and absence of inhibitors, respectively (OD min^{-1}), and $[I]$ is the inhibitor's concentration (μM).

RESULTS AND DISCUSSION

Spectral Study. Twelve new derivatives of phosphoramide analogues were synthesized (Scheme 1) and characterized by ^{31}P , ^{13}C , and ^1H NMR and IR spectroscopy. The ^{31}P NMR chemical shift was revealed to be in the range of -2.05 (34) to 11.67 ppm (28), and the ^{13}C NMR chemical shift of carbonyl group was in the range of 175.93 (4) to 176.88 ppm (2). The phosphorus–carbon coupling constant $^3J(\text{P},\text{C})$ appeared as a doublet peak at the range of 4.3 (35) to 8.5 Hz (29). The $\text{P}=\text{O}$ and $\text{C}=\text{O}$ vibrational frequencies of the compounds appeared in the ranges 1155–1212 cm^{-1} and 1670–1702 cm^{-1} , respectively. In all the synthesized compounds, the $\text{N}-\text{H}_{\text{amine}}$ stretching vibrations (3085–3390 cm^{-1}) appeared at higher frequencies than those of the $\text{N}-\text{H}_{\text{amide}}$ vibrational bands (3085–3125 cm^{-1}). Other characteristic fundamentals for these species are $\text{N}-\text{P}$ stretching modes, typically observed at the frequency values around 827–888 cm^{-1} . These values are in good agreement with the reported vibrational data for the related compounds.⁴⁰

Prediction of Insecticide Potential. PASS software predicts 900 types of biological activities based on the structural formula. The default list of predictable biological activities (P_a) includes the main and side pharmacological effects, molecular mechanisms, and specific toxicities.⁴¹ Insecticide potential and anti-AChE activities of 23 Ace analogues have been obtained by using the PASS software, and the results are summarized in Table 1. The comparison of experimental data and prediction of anti-AChE activities are shown in Figure 2a. Also, the plot of probable insecticide potential of compounds 1–12 against anti-AChE activity (Figure 2b) indicates that there is an agreement between both of them.

Structural Analysis of Docking. The interactions between Ace derivatives and AChE receptor were achieved by molecular docking, which can facilitate the selection of appropriate molecular parameters in the subsequent QSAR studies.⁴² The receptor site of AChE consists of at least four subsites: (i) anionic subsites, (ii) a steratic site, (iii) an oxyanion–hole, and (iv) acyl–pocket.^{6,43} Docking of compound 2 was used as a template because it has the highest inhibition potency against the AChE enzyme (Table 1). As shown in Figure 3, hydrogen bonding and hydrophobic interactions are the predominant interactions between the compound 2 and AChE enzyme. H-Bonds formation in the esteratic site was found to occur between the amidic hydrogen and the nitrogen of the imidazole of His440 and also between the amidic nitrogen and the $\text{H}-\text{O}$ functional group of Ser200. In the oxyanion–hole site, H-bonds arose between $\text{P}=\text{O}$ oxygen and the NH functional groups of Gly118 and Gly119. Moreover, the hydrophobic interactions with appropriate distance were created between the $\text{C}=\text{O}$ carbon and Trp84.

QSAR Analysis. Several models have been suggested to explain the inhibition mechanism of AChE including ab initio analysis by Sokalski⁵ and Singh.^{6,7} These studies were not successful because the electronic and structural properties of Ace analogues have not been evaluated by regression models. Here, we explain the inhibition mechanism of human AChE by experimental and theoretical QSAR models.

Experimental quantities-based QSAR analysis: an optimal QSAR equation based on experimental data (δ , $\log P$, and M_r) shown in Table 1 was obtained for 23 compounds as follows:

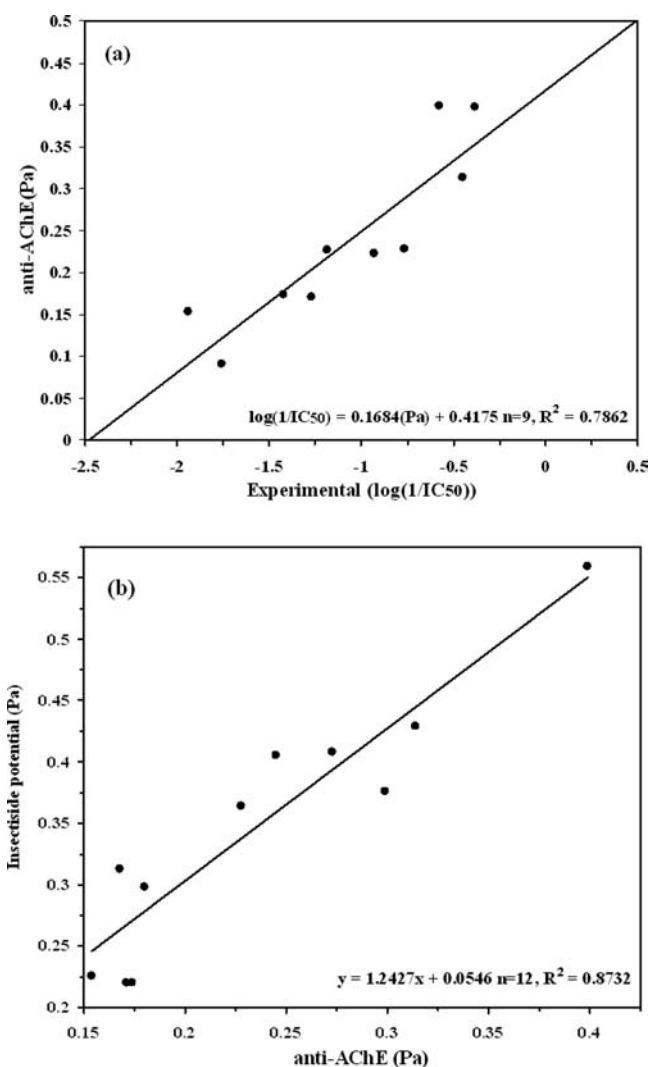


Figure 2. The plot of experimental values against prediction of anti-AChE activity (a); the plot of probable insecticide potential against probable anti-AChE activity of compounds 1–12 (b).

$$\log(1/IC_{50}) = -0.538\log P - 0.148\delta(^{31}\text{P}) + 0.222\delta(^{13}\text{C}) + 1.330\delta(^1\text{H}) + 0.284\text{Mr} + 49.441$$

$$n = 17; R^2 = 0.903; R_{\text{adj}}^2 = 0.859; S_{\text{reg}} = 0.486; r = 0.26, F_{\text{statistic}} = 20.546$$

(5)

where n is the number of compounds, r is the correlation coefficient, R^2 is the determination coefficient, R_{adj}^2 is the adjusted determination coefficient, S_{reg} is the standard deviation of regression, and $F_{\text{statistic}}$ is the Fisher statistic.³⁸ Equation 5 shows that $\log(1/IC_{50})$ is dependent on the electronic descriptors, particularly $\delta(^1\text{H})$, more than the hydrophobic ($\log P$) and molar refractivity (Mr) parameters with high determination coefficient ($R^2 = 0.903$) and low residual ($S_{\text{reg}} = 0.486$).

By replacement of experimental variables with the descriptors derived from the DFT calculations (Table 2), the following equation is produced.

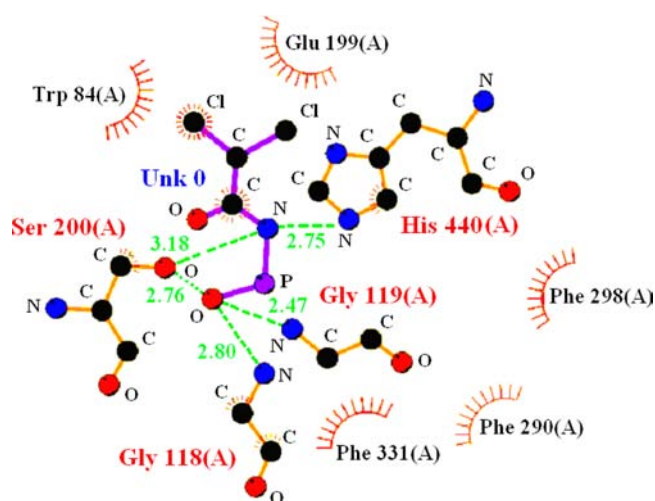


Figure 3. Hydrogen-bonding and hydrophobic interaction between compound 2 and AChE in the binding site (blue dot connected to a black dot with a purple line, ligand bond; blue dot connected to a black dot with a gold line, nonligand bond; blue dot connected to a red dot by a dotted green line, hydrogen bond and its length; amino acid residues with red rays, nonligand residues involved in hydrophobic contacts; black dot with red rays, corresponding atoms involved in hydrophobic contacts).

$$\begin{aligned} \log(1/IC_{50}) = & +0.121\mu + 0.574Q_C + 89.545Q_N \\ & + 4.904PL_{\text{P=O}} + 49.513PPL_{\text{C=O}} + 91.730PL_{\text{N-H}} \\ & + 40.986E_{\text{HOMO}} - 4.656E_{\text{LUMO}} + 67.733\Delta E_{\text{L-H}} \\ & - 10.660\omega + 0.007\text{Mv} - 62.072 \\ n = 17; R^2 = 0.991; R_{\text{adj}}^2 = 0.972; S_{\text{reg}} = 0.153; r = 0.55, F_{\text{statistic}} = 51.505 \end{aligned}$$

(6)

Comparison of the correlation coefficient of $PL_{\text{N-H}}$ (+91.730) with random error (−62.072) demonstrates that this descriptor can play a crucial function in the interaction of the compounds with AChE. The high values of correlation ($|r| = 0.55$) and variance inflation factor ($\text{VIF} > 10$) lead to refusing the calculation of IC_{50} . The best way to deal with such a problem is to calculate variance inflation factor (VIF). We calculated VIF, which is a measure of multicollinearity, for each of the parameters involved in models. The VIF is defined as $1/(1 - R_i^2)$, where R_i is the multiple correlation coefficient of the i th independent variable on all of the other independent variables. A VIF of 10 or more (no upper limit is defined) for large data sets indicates a collinearity problem. For small data sets, even VIFs of five or more (here also no upper limit is defined) can signify collinearity. On the other hand, the VIF value greater than 10 (Table 3) is associated with multicollinearity problem. Therefore, the variables with a high VIF are candidates for exclusion from the model.⁴⁴ To clarify this problem, use of the PCA method is needed.⁴⁵

PCA-QSAR Equation. Fisher's weight approach is a method for the reduction and selection of the best descriptors which have high correlation between the variables and principal components. PC⁴⁶ eqs 7a and 7b were obtained with eight variables from among 17 descriptors:

Table 3. VIF^a/Tolerance^b Values of Experimental and Theoretical QSAR Equations

independent variables	experimental		theoretical	
	eq 1	eq 2	eq 4	eq 5
log P	1.585 ^a /0.631 ^b			
δ(³¹ P)	2.005/0.499			
δ(¹³ C ₁)	2.797/0.358			
δ(¹ H ₁)	2.997/0.334			
Mr	2.428/0.412			
Q _P			447.703/0.002	2.923/0.342
Q _{N(1)}		8.202/0.122	19.534/0.051	
Q _{C(1)}		182.003/0.005	551.545/0.002	3.815/0.262
PL _{P=O}		164.749/0.006	15.077/0.066	
PL _{C=O}		93.231/0.011	32.504/0.031	
PL _{N-H}		160.809/0.006	12.925/0.077	8.413/0.119
E _{HOMO}		383.745/0.003		6.869/0.146
E _{LUMO}		6.917/0.145		
Δ _{L-H}		118.312/0.008		
ω		2.032/0.492		
μ		6.317/0.158	2.842/0.352	4.240/0.236
Mv		23.788/0.042	17.447/0.057	10.643/0.094

^aVIF = 1/(1 - R_i²), where R_i is the multiple correlation coefficient of the *i*th independent variable on all of the other independent variables.
^bTolerance = 1/VIF.

$$PC_1 = +0.439Q_P - 0.273Q_C - 0.441PL_{P=O} + 0.126PL_{C=O} + 0.443PL_{N-H} + 0.372E_{HOMO} - 0.093\mu + 0.423Mv \quad (7a)$$

$$PC_2 = -0.100Q_P - 0.524Q_C + 0.104PL_{P=O} + 0.645PL_{C=O} - 0.001PL_{N-H} - 0.285E_{HOMO} - 0.426\mu - 0.159Mv \quad (7b)$$

The main variables were found from the principle scores of the normalized eigenvalue of the two principal components. The results showed that the first and second factor PC on the total variance were 59.5% and 24.3%, respectively. Also, from the above equations, it was deduced that the electronic parameters (Q_P, Q_C, PL_{C=O}, PL_{N-H}, and E_{HOMO}) are predominated from those related to structural parameters (μ and Mv). Figure 4 shows the score and a loading plot of PC₁ × PC₂. The compounds are grouped into two main regions: high

activity (upper half of PC₂) and low activity (lower half of PC₂). The compounds that exhibit log(1/IC₅₀) values greater than -0.931 with aliphatic carboxamide were grouped as high activity, while the aromatic carboxamide were grouped as low activity with log(1/IC₅₀) values lower than -0.931. PC₁ exclusively separates the score plot on the foundation of structural differences. The compounds with substituents N(CH₂)₄O, NH-N(CH₂)₄O and NH-N(CH₂)₅ were located in the right side, and the rest with substituent Cl were situated in the left side. The MLR was performed using these eight descriptors, which resulted following equation:

$$\begin{aligned} \log(1/IC_{50}) &= -0.061\mu + 19.143Q_P + 2.449Q_C \\ &+ 14.000PL_{P=O} + 18.058PL_{C=O} + 29.058PL_{N-H} \\ &- 42.123E_{HOMO} - 0.005Mv + 38.601 \\ n &= 19; R^2 = 0.723; R_{adj}^2 = 0.501; S_{reg} = 0.854; r \\ &= 0.45, F_{statistic} = 3.257 \end{aligned} \quad (8)$$

The low determination coefficient (R² = 0.723) and high residuals (S_{reg} = 0.854) with high variance inflation factor (VIF) > 10 (Table 3) determined the multicollinearity problem. The improvement in the eq 8 was carried out by omitting the compounds 20 and 21 from tested compounds and replacing the Q_P with Q_C and PL_{P=O} with PL_{C=O}. Multiple regressions performed using these six parameters yielded the following model with increasing the R² = 0.949 and decreasing the S_{reg} = 0.352.

$$\begin{aligned} \log(1/IC_{50}) &= -0.651\mu + 3.051Q_P + 1.309Q_C \\ &+ 52.865PL_{N-H} - 23.916E_{HOMO} - 0.031Mv + 62.176 \\ n &= 17; R^2 = 0.949; R_{adj}^2 = 0.918; S_{reg} = 0.352; r \\ &= 0.29, F_{statistic} = 30.850 \end{aligned} \quad (9)$$

The correlating parameters have VIF < 10, and thus there is no colinearity problem (Table 3). In this equation, PL_{N-H} with

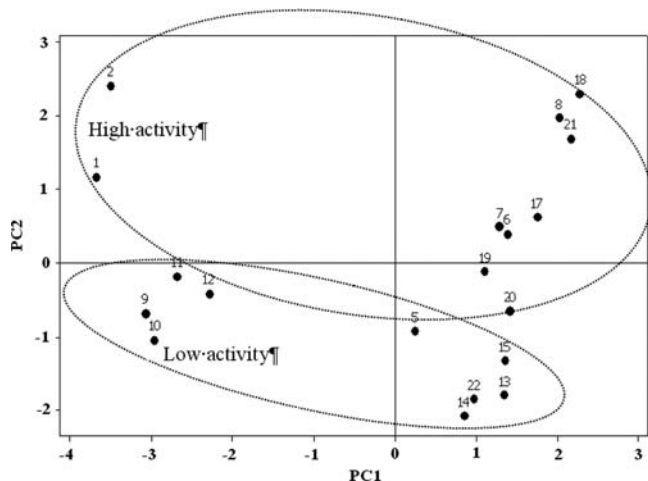


Figure 4. PCA score plot for 19 Ace derivatives.

Table 4. Results from the External Validation Step Performed with the Real Model with the Selected Test Set from the Auxiliary Model

no.	$\delta(^{31}\text{P})$	$\delta(^{13}\text{C}_1)$	$\delta(^1\text{H}_1)$	Q_p	Q_c	μ	$\text{PL}_{\text{N-H}}$	E_{HOMO}	Mv	$\log(1/\text{IC}_{50})_{\text{expt}}$	$\log(1/\text{IC}_{50})_{\text{pred}}^a$	res^b
3	8.08	160.30	9.94	1.824	0.655	5.700	-1.421	-0.320	114.294	-0.580	-0.175	0.405
4	7.42	157.50	10.24	1.815	0.607	5.516	-1.416	-0.329	108.614	-0.380	0.073	0.453
16	10.81	166.08	8.82	2.365	0.675	7.096	-1.376	-0.248	228.264	-1.757	-2.101	-0.344
23	2.49	167.81	9.08	2.315	0.676	8.003	-1.373	-0.247	255.507	-0.290	-1.719	-1.429
27	1.40	171.31	9.25	2.342	0.707	6.488	-1.386	-0.256	231.691	-0.555	-0.855	-0.300
28	11.76	171.30	8.91	2.365	0.704	7.916	-1.394	-0.248	240.775	-0.969	-1.059	-0.090
29	6.10	171.97	9.31	2.366	0.703	8.148	-1.376	-0.243	229.086	-0.644	-0.922	-0.278
30	9.19	171.77	8.86	2.362	0.703	8.841	-1.393	-0.249	231.042	-0.331	-1.057	-0.726
31	8.10	172.25	9.21	2.360	0.705	6.779	-1.399	-0.252	212.399	0.522	0.386	0.136

^aPredictive activities were calculated using the QSAR model. ^bResidual for molecule is the difference between the experimental property and predicted property.

the coefficient of +52.865 has the highest contribution to $\log(1/\text{IC}_{50})$; it implies that the polarizability plays an effective function in the interaction mechanism of the Ace analogous with AChE enzyme. The positive signs of $\text{PL}_{\text{N-H}}$ in $\log(1/\text{IC}_{50})$ reveals the compound with higher polarizability discloses the higher toxicity against AChE enzyme. Equation 9 is a fitting model, but its validity and the predictive ability of QSAR model must be evaluated by the LOO cross-validation method.

Validation of MLR-QSAR Model. The LOO cross-validation method was used for training sets to select the optimum values of parameters. This procedure consists three stage: (i) removing one sample from the training set, (ii) constructing the equation on the basis of only the remaining training data, and (iii) testing of the model on the removed and innovative samples.⁴⁷ Random selection was used separately to divide the whole data set into training set and test set. A set of 19 compounds (PS) was used as a training set for QSAR modeling. The remaining nine compounds (3, 4, 16, and 23 as PS and 27–31 as NS) were adopted as a test set for validating the QSAR model. Considering the balance of the QSAR quality and the number of employed quantum-chemical descriptors, an optimal equation was achieved for 17 compounds in the training set by MLR analysis as follows:

$$\log(1/\text{IC}_{50}) = -0.651\mu + 3.051Q_p + 1.309Q_c + 52.865\text{PL}_{\text{N-H}} - 23.916E_{\text{HOMO}} - 0.031\text{Mv} + 62.176$$

$$n = 17; R^2 = 0.949; R_{\text{adj}}^2 = 0.918; S_{\text{reg}} = 0.352; r = 0.29;$$

$$F_{\text{statistic}} = 30.850; q^2 = 0.940; P < 0.0001 \quad (10)$$

where q^2 is the square of LOO cross-validation coefficient. A good QSAR model has characters of large F , small r , and S_{reg} low P -value ($P < 0.001$), and R^2 and q^2 values close to 1),⁴⁸ so the above established eq 10 shows appropriate statistical quality. Moreover, a new equation is proposed to determine the outliers using LOO cross-validation coefficient q_{n-i}^2 which is equal to the q^2 of compound i computed by the new cross-validation procedure after leaving this datum point out from n compounds. The compound with unduly high q_{n-i}^2 value can be considered as an outlier, and the compound with the low value can be indicated as an influential point.⁴⁹ Compound 10 has too large q_{n-i}^2 value in the training set, so this compound can be confirmed to be the outlier. After omitting compound 10, an optimal model is obtained:

$$\log(1/\text{IC}_{50}) = -0.646\mu + 3.477Q_p + 1.378Q_c + 57.272\text{PL}_{\text{N-H}} - 25.476E_{\text{HOMO}} - 0.033\text{Mv} + 67.019$$

$$n = 16; R^2 = 0.955; R_{\text{adj}}^2 = 0.925; S_{\text{reg}} = 0.331; r = 0.20;$$

$$F_{\text{statistic}} = 31.970; q^2 = 0.955; P < 0.0001 \quad (11)$$

Equation 11 with larger R^2 and q^2 values indicates the best statistical quality in comparison to eq 10. To check and consider the validity of eq 11, we selected our previous omitted nine compounds as the test set, which the dependent and independent variables with their residuals of test set compounds are shown in Table 4. Table 4 and particularly residuals data show that the inhibition results are the same in the empirical method and prediction technique. Figure 5 indicates that the predicted values of $\log(1/\text{IC}_{50})$ are in a good agreement with the experimental ones. The integrity was validated by determination coefficient ($R^2 = 0.835$) and residuals between the training and testing sets. To show the interrelationship between independent variables the correlation matrix was used and no obvious multicollinearity was found

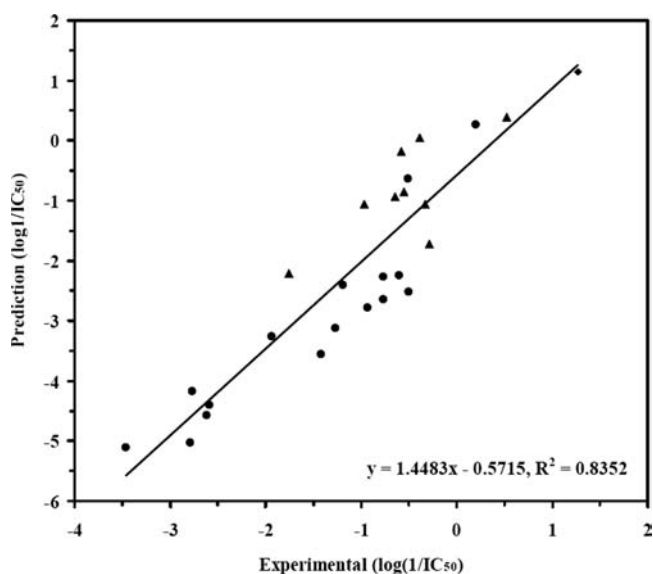


Figure 5. Plot of predicted activities versus experimental ones for the QSAR model (eqs 7), in which 19 compounds are the training set (●) and correspondingly nine compounds are the test set (▲).

and the results are presented in Table 5. Table 5 shows that independent variables are correlated with each other regardless

Table 5. Correlation Matrix for $\log(1/IC_{50})$ and Selected Parameters in eqs 7

	μ	PL_{N-H}	Q_P	Q_C	E_{HOMO}	Mv
μ	1.000					
PL_{N-H}	-0.260	1.000				
Q_P	-0.234	0.935	1.000			
Q_C	0.527	-0.528	-0.420	1.000		
E_{HOMO}	0.081	0.723	0.787	0.076	1.000	
Mv	-0.276	0.881	0.862	-0.310	0.844	1.000

of the dependent variable. A high interrelationship was observed between Q_P and PL_{N-H} ($r = +0.935$), and a low interrelationship was observed between Q_C and E_{HOMO} ($r = +0.026$). The effect of dipole moment in modulating inhibition activity against AChE enzyme may be due to the presence of carbonyl group ($C^{\delta+}-O^{\delta-}$), where permanent polarization was seen due to electronegativity difference between the atoms. Therefore, the carbonyl oxygen was able to making binding interactions with the amino acid present at the target site, and docking analysis confirmed this result (Figure 3). A hydrophobic interaction was created between the $C=O$ carbon and Trp84. Moreover, hydrogen bonds were occurred between the $N-H$ and $P=O$ functional groups of compounds with the esteratic site (Ser200 and His440) and the oxyanion-hole (Gly118 and Gly119), respectively. Molecular docking analysis and QSAR modification models were used for determining the inhibition mechanism of human AChE by 35 Ace analogues with the general skeleton $RC(O)-NH-P(O)X_1X_2$. Docking analysis showed that a hydrophobic interaction is created between the $C=O$ functional group and Trp84. Also, the $N-H$ and $P=O$ functional groups of compounds interact through hydrogen bonding with the esteratic and oxyanion-hole sites, respectively. The optimal MLR-QSAR models based on the experimental and theoretical calculations revealed that the electronic parameters are the most effective variables in the interaction mechanism of AChE and Ace derivatives. PCA-QSAR equations of eight main variables indicated that the electronic descriptors (Q_P , Q_C , $PL_{C=O}$, $PL_{N=O}$, PL_{N-H} , and E_{HOMO}) are dominant in comparison with the structural descriptors (μ and Mv). Furthermore, the problem of multicollinearity of DFT-QSAR models was solved by using the PCA analysis. DFT-QSAR model ($R^2 = 0.949$ and $VIF < 10$) revealed that the PL_{N-H} descriptor contribute an important function in the inhibition mechanism. The validity and the integrity of this model were confirmed by LOO cross-validation method with $q^2 = 0.940$, $R^2 = 0.835$, and low residuals between the training and testing sets. The correlation matrix of DFT-QSAR model confirmed that the $C=O$ group and combination of the $N-H$ and $P=O$ groups of Ace analogues inhibit the human AChE enzyme via hydrophobic interaction and hydrogen-bonding, respectively. Finally, it can be concluded that the experimental results in QSAR model are in an excellent agreement with the theoretical calculations to clarify the net charge of functional groups as the most effective descriptors in inhibition of AChE.

■ ASSOCIATED CONTENT

■ Supporting Information

Spectral data as indicated in the text relative to phosphoic triamides (24–35). This material is available free of charge via the Internet at <http://pubs.acs.org>.

■ AUTHOR INFORMATION

■ Corresponding Author

*Phone: +98 21 82883443. Fax: +98 218006544. E-mail: gholi_kh@modares.ac.ir.

■ Funding

The financial support of Tarbiat Modares University's Research Council is gratefully acknowledged.

■ Notes

The authors declare no competing financial interest.

■ ABBREVIATIONS USED

Ace, acephate; AChE, acetylcholinesterase; HOMO, highest occupied molecular orbital; LUMO, lowest unoccupied molecular orbital; PL, polarizability; Mv, molecular volume; Mr, molar refractivity; PCA, principal component analysis; QSAR, quantitative structure-activity relationships; LOO, leave-one-out; MLR, multiple linear regression; DFT, density function theory; VIF, variance inflation factor; SPSS, statistical package for social scientists; PASS, prediction of activity spectrum for substances; PDB, Protein Data Bank; NPA, natural population analysis

■ REFERENCES

- O'Brien, R. D. Mode of Action of Insecticides, Binding of Organophosphates to Cholinesterases. *J. Agric. Food Chem.* **1963**, *11*, 163–166.
- Singh, A. K. Kinetic analysis of inhibition of brain and red blood cell acetylcholinesterase and plasma cholinesterase by acephate or methamidophos. *Toxicol. Appl. Pharmacol.* **1985**, *81*, 302–309.
- Singh, A. K. *Toxicol. Ind. Health* **1990**, *6*, 551–570.
- Ghadimi, S.; Mousavi, S. L.; Rahnama, Z.; Rahimi, M. Synthesis and Characterization of *O,S*-Dimethylphosphoramidothioate and *N*-Acetyl *O,S*-Dimethylphosphoramidothioate. *Phosphorus, Sulfur Silicon Relat. Elem.* **2010**, *185*, 347–354.
- Kazimierowicz, E. D.; Sokalski, W. A.; Leszczynski, J. Gas-Phase Mechanisms of Degradation of Hazardous Organophosphorus Compounds: Do They Follow a Common Pattern of Alkaline Hydrolysis Reaction As in Phosphotriesterase? *J. Phys. Chem. B* **2008**, *112*, 9982–9991.
- Singh, A. K.; White, T.; Spassova, D.; Jiang, Y. Physicochemical, Molecular-Orbital and Electronic Properties of Acephate and Methamidophos. *Comp. Biochem. Physiol., Part C: Toxicol. Pharmacol.* **1998**, *119*, 107–117.
- Singh, A. K. Quantitative structure-activity relationships for phosphoramidothioate toxicity in housefly. *Comp. Biochem. Physiol., Part C: Toxicol. Pharmacol.* **1999**, *123*, 241–255.
- Soderholm, A. A.; Lehtovuori, P. T.; Nyronen, T. H. Three-Dimensional Structure-Activity Relationships of Nonsteroidal Ligands in Complex with Androgen Receptor Ligand-Binding Domain. *J. Med. Chem.* **2005**, *48*, 917–925.
- Sippl, W. Development of biologically active compounds by combining 3D QSAR and structure-based design methods. *J. Comput.-Aided Mol. Des.* **2002**, *16*, 825–830.
- Amadasi, A.; Mozzarelli, A.; Meda, C.; Maggi, A.; Cozzini, P. Identification of Xenoestrogens in Food Additives by an Integrated in Silico and in Vitro Approach. *Chem. Res. Toxicol.* **2009**, *22*, 52–63.
- Li, F.; Wua, H.; Li, L.; Li, X.; Zhao, J.; Peijnenburg, W. G. M. Docking and QSAR study on the binding interactions between

polycyclic aromatic hydrocarbons and estrogen receptor. *Ecotoxicol. Environ. Saf.* **2012**, *80*, 273–279.

(12) De melo, E. B. Multivariate SAR/QSAR of 3-aryl-4-hydroxyquinolin-2(1H)-one derivatives as type I fatty acid synthase (FAS) inhibitors. *Eur. J. Med. Chem.* **2010**, *45*, 5817–5826.

(13) Pillai, A. D.; Rani, S.; Rathod, P. D.; Xavier, F. P.; Vasu, K. K.; Padhd, H.; Sudarsanam, V. QSAR studies on some thiophene analogs as anti-inflammatory agents: enhancement of activity by electronic parameters and its utilization for chemical lead optimization. *Bioorg. Med. Chem.* **2005**, *13*, 1275–1283.

(14) Soltani, S.; Abolhasani, H.; Zarghi, A.; Jouyban, A. QSAR analysis of diaryl COX-2 inhibitors: comparison of feature selection and train-test data selection methods. *Eur. J. Med. Chem.* **2010**, *45*, 2753–2760.

(15) Wang, N. C. Y.; Venkatapathy, R.; Bruce, R. M.; Moudgal, C. Development of Quantitative Structure–Activity Relationship Models to Predict the Carcinogenic Potency of Chemicals. II: Using Oral Slope Factor as a Measure of Carcinogenic Potency. *Regul. Toxicol. Pharmacol.* **2011**, *59*, 215–226.

(16) Gholivand, K.; Abdollahi, M.; Mojahed, F.; Alizadegan, A. M.; Dehghan, G. Acetylcholinesterase/butyrylcholinesterase inhibition activity of some new carbacylamidophosphate derivatives. *J. Enzyme Inhib. Med. Chem.* **2008**, 1–11.

(17) Gholivand, K.; Alizadegan, A. M.; mojahed, F.; Dehghan, G.; Mohammadirad, A.; Abdollahi, M. Some new carbacylamidophosphates as inhibitors of acetylcholinesterase and butyrylcholinesterase. *Z. Naturforsch.* **2008**, *63c*, 241–250.

(18) Gholivand, K.; Alizadegan, A. M.; Firoozi, A. A.; Khajeh, K.; Naderimanesh, H.; Bijanzadeh, H. R. Anticholinesterase activity of some major intermediates in carbacylamidophosphate synthesis: preparation, spectral characterization and inhibitory potency determination. *J. Enzyme Inhib. Med. Chem.* **2006**, *21*, 105–111.

(19) Gholivand, K.; Mojahed, F.; Alizadegan, A. M. Synthesis and characterization of novel carbacylamidophosphate derivatives: Crystal structures of $(\text{CF}_3)\text{C}(\text{O})\text{NHP}(\text{O})(\text{NC}_6\text{H}_{12})_2$, $(p\text{-Br-C}_6\text{H}_4)\text{C}(\text{O})\text{NHP}(\text{O})(\text{NC}_6\text{H}_{12})_2$ and $(p\text{-Cl-C}_6\text{H}_4)\text{C}(\text{O})\text{NHP}(\text{O})(\text{NC}_6\text{H}_{12})_2$. *Pol. J. Chem.* **2007**, *81*, 393–402.

(20) Lagunin, A.; Stepanchikova, A.; Filimonov, D.; Poroikov, V. PASS: prediction of activity spectra for biologically active substances. *Bioinformatics Appl. Notes* **2000**, *16*, 747–748.

(21) Morris, G. M.; Goodsell, D. S.; Halliday, R. S.; Huey, R.; Hart, W. E.; Belew, R. K.; Olson, A. J. Automated docking using a Lamarckian genetic algorithm and an empirical binding free energy function. *J. Comput. Chem.* **1998**, *19*, 1639–1662.

(22) Reed, A. E.; Curtiss, L. A.; Weinhold, F. Intermolecular interactions from a natural bond orbital, donor–acceptor viewpoint. *Chem. Rev.* **1988**, *88*, 899–926.

(23) Carpenter, J. E.; Weinhold, F. Analysis of the geometry of the hydroxymethyl radical by the “different hybrids for different spins” natural bond orbital procedure. *J. Mol. Struct. (Theochem)* **1988**, *169*, 41–46.

(24) Frisch, M. J.; Trucks, G. W.; Schlegel, H. B.; Scuseria, G. E.; Robb, M. A.; Cheeseman, J. R.; Montgomery, J. A.; Vreven, T.; Kudin, K. N.; Burant, J. C.; Millam, J. M.; Iyengar, S. S.; Tomasi, J.; Barone, V.; Mennucci, B.; Cossi, M.; Scalmani, G.; Rega, N.; Petersson, G. A.; Nakatsuji, H.; Hada, M.; Ehara, M.; Toyota, K.; Fukuda, R.; Hasegawa, J.; Ishida, M.; Nakajima, T.; Honda, Y.; Kitao, O.; Nakai, H.; Klene, M.; Li, X.; Knox, J. E.; Hratchian, H. P.; Cross, J. B.; Bakken, V.; Adamo, C.; Jaramillo, J.; Gomperts, R.; Stratmann, R. E.; Yazyev, O.; Austin, A. J.; Cammi, R.; Pomelli, C.; Ochterski, J. W.; Ayala, P. Y.; Morokuma, K.; Voth, G. A.; Salvador, P.; Dannenberg, J. J.; Zakrzewski, V. G.; Dapprich, S.; Daniels, A. D.; Strain, M. C.; Farkas, O.; Malick, D. K.; Rabuck, A. D.; Raghavachari, K.; Foresman, J. B.; Ortiz, J. V.; Cui, Q.; Baboul, A. G.; Clifford, S.; Cioslowski, J.; Stefanov, B. B.; Liu, G.; Liashenko, A.; Piskorz, P.; Komaromi, I.; Martin, R. L.; Fox, D. J.; Keith, T.; Al-Laham, M. A.; Peng, C. Y.; Nanayakkara, A.; Challacombe, M.; Gill, P. M. W.; Johnson, B.; Chen, W.; Wong, M. W.; Gonzalez, C.; Pople, J. A. *Gaussian 03*, revision D.01; Gaussian, Inc.: Wallingford CT, 2005.

(25) *SPSS for Windows*, version 10.05; SPSS Inc.: Bangalore, India, 1999.

(26) Hansch, C.; Fujita, T. p - σ - π Analysis. A Method for the Correlation of Biological Activity and Chemical Structure. *J. Am. Chem. Soc.* **1964**, *86*, 1616–1626.

(27) Jung, M.; Tak, J.; Lee, Y.; Jung, Y. Quantitative structure–activity relationship (QSAR) of tacrine derivatives against acetylcholinesterase (AChE) activity using variable selections. *Bioorg. Med. Chem. Lett.* **2007**, *17*, 1082–1090.

(28) Parr, R. G.; Szentpaly, L. V.; Liu, S. Electrophilicity Index. *J. Am. Chem. Soc.* **1999**, *121*, 1922–1924.

(29) Hua, R.; Doucet, J. P.; Delamar, M.; Zhang, R. QSAR models for 2-amino-6-arylsulfonylbenzonnitriles and congeners HIV-1 reverse transcriptase inhibitors based on linear and nonlinear regression methods. *Eur. J. Med. Chem.* **2009**, *44*, 2158–2171.

(30) Ghadimi, S.; Valmoozi, A. A. E.; Pourayoubi, M.; Samani, K. A. Structure–activity study of phosphoramido acid esters. *J. Enzyme Inhib. Med. Chem.* **2008**, *23* (4), 556–561.

(31) Sharma, S. K.; Kumar, P.; Narasimhan, B.; Ramasamy, K.; Mani, V.; Mishra, R. K.; Majeed, A. A. Synthesis, antimicrobial, anticancer evaluation and QSAR studies of 6-methyl-4-[1-(2-substituted-phenylamino-acetyl)-1H-indol-3-yl]-2-oxo/thioxo-1,2,3,4-tetrahydropyrimidine-5-carboxylic acid ethyl esters. *Eur. J. Med. Chem.* **2012**, *48*, 16–25.

(32) Viswanadhan, V. N. Atomic Physicochemical Parameters for Three Dimensional Structure Directed Quantitative Structure–Activity Relationships. 4. Additional Parameters for Hydrophobic and Dispersive Interactions and Their Application for an Automated Superposition of Certain Naturally Occurring Nucleoside Antibiotics. *J. Chem. Inf. Comput. Sci.* **1989**, *29*, 163–172.

(33) Saric, M. M.; Mornar, A.; Crnjevic, T. B.; Jasprica, I. Experimental and Calculation Procedures for Molecular Lipophilicity: A Comparative Study for 3,3'-(2-Methoxybenzylidene)bis(4-hydroxycoumarin). *Croat. Chem. Acta.* **2004**, *77*, 367–370.

(34) Malta, V. R. S.; Pinto, A. V.; Molffeta, F. A.; Honório, K. M.; de Simone, C. A.; Pereira, M. A.; Santos, R. H. A.; da Silva, A. B. F. The influence of electronic and steric effects in the structure–activity relationship (SAR) study of quinone compounds with biological activity against *Trypanosoma cruzi*. *J. Mol. Struct. (Theochem)* **2003**, *634*, 271–280.

(35) Pinto, M. F. S.; Romero, O. A. S.; Pinheiro, J. C. Pattern recognition study of structure–activity relationship of halophenols and halonitrophenols against fungus *T. mentagrophytes*. *J. Mol. Struct. (Theochem)*. **2001**, *539*, 303–310.

(36) De, K.; Sengupta, C.; Roy, K. QSAR modeling of globulin binding affinity of corticosteroids using AM1 calculations. *Bioorg. Med. Chem.* **2004**, *12*, 3323–3332.

(37) Tetko, I. V.; Tanchuk, V. Y.; Villa, A. E. Prediction of n -Octanol/Water Partition Coefficients from PHYSPROP Database Using Artificial Neural Networks and E-State Indices. *J. Chem. Inf. Comput. Sci.* **2001**, *41*, 1407–1421.

(38) Roy, D. R.; Sarkar, U.; Chattaraj, P. K.; Mitra, A.; Padmanabhan, J.; Parthasarathi, R.; Subramanian, V.; Van Damme, S.; Bultinck, P. Analyzing toxicity through electrophilicity. *Mol. Divers.* **2006**, *10*, 119–131.

(39) Schuurmann, G.; Ebert, R. U.; Chen, J. W.; Wang, B.; Kuhne, R. External Validation and Prediction Employing the Predictive Squared Correlation Coefficient—Test Set Activity Mean vs Training Set Activity Mean. *J. Chem. Inf. Model.* **2008**, *48*, 2140–2145.

(40) Gholivand, K.; Hosseini, Z.; Farshadian, S.; Naderi-Manesh, H. Synthesis, characterization, oxidative degradation, antibacterial activity and acetylcholinesterase/butyrylcholinesterase inhibitory effects of some new phosphorus(V) hydrazides. *Eur. J. Med. Chem.* **2010**, *45*, 5130–5139.

(41) Geronikaki, A. A.; Dearden, J. C.; Filimonov, D.; Galaeva, I.; Garibova, L.; Glorizova, T.; Kranjceva, V.; Lagunin, A.; Macaev, F. Z.; Molodavkin, G.; Poroikov, V.; Pobrebnoi, S. I.; Shepeli, F.; Voronina, T.; Tsitlakido, M.; Vald, L. Design of new cognition enhancers: from computer prediction to synthesis and biological evaluation. *J. Med. Chem.* **2004**, *47*, 2870–2876.

(42) Correa-Basurto, J.; Flores-Sandoval, C.; Marin-Cruz, J.; Rojo-Dominguez, A.; Espinoza-Fonseca, L. M.; Trujillo-Ferrara, J. G. Docking and quantum mechanic studies on cholinesterases and their inhibitors. *Eur. J. Med. Chem.* **2007**, *42*, 10–19.

(43) Hosa, N. A.; Radic, Z.; Tsigeling, I.; Berman, H. A.; Quinn, D. M.; Taylor, P. Aspartate 74 as a primary determinant in acetylcholinesterase governing specificity to cationic organophosphonates. *Biochemistry*. **1996**, *35*, 10995–11004.

(44) Singh, J.; Shaik, B.; Singh, S.; Agrawal, V. K.; Khadikar, P. V.; Deeb, O.; Supuran, C. T. Comparative QSAR Study on Para-Substituted Aromatic Sulphonamides as CAII Inhibitors: Information versus Topological (Distance-Based and Connectivity) Indices. *Chem. Biol. Drug. Des.* **2008**, *71*, 244–259.

(45) Pillai, A. D.; Rani, S.; Rathod, P. D.; Xavier, F. P.; Vasu, K. K.; Padh, H.; Sudarsanam, V. QSAR studies on some thiophene analogs as anti-inflammatory agents: enhancement of activity by electronic parameters and its utilization for chemical lead optimization. *Bioorg. Med. Chem.* **2005**, *13*, 1275–1283.

(46) Molfetta, F. A.; Bruni, A. T.; Honório, K. M.; da Silva, A. B. F. A structure–activity relationship study of quinone compounds with trypanocidal activity. *Eur. J. Med. Chem.* **2005**, *40*, 329–338.

(47) Hua, R.; Doucet, J. P.; Delamar, M.; Zhang, R. QSAR models for 2-amino-6-arylsulfonylbenzimidazoles and congeners HIV-1 reverse transcriptase inhibitors based on linear and nonlinear regression methods. *Eur. J. Med. Chem.* **2009**, *44*, 2158–2171.

(48) Liao, S. Y.; Chen, J. C.; Qian, L.; Shen, Y.; Zheng, K. C. QSAR, action mechanism and molecular design of flavone and isoflavone derivatives with cytotoxicity against HeLa. *Eur. J. Med. Chem.* **2008**, *43*, 2159–2170.

(49) Chen, J. C.; Shen, Y.; Liao, S. Y.; Chen, L. M.; Zheng, K. C. DFT-based QSAR study and molecular design of AHMA derivatives as potent anticancer agents. *Int. J. Quantum Chem.* **2006**, *107*, 1468–1478.